Table DR1 Page 1 of 4

Station	Lat	Lon	dt	phi	events	error dt	error phi	Zone	Event IDs
BB030	42.95	-126.93	1.8	-66	1	0.2	3	blanco	28
BB060	42.86	-126.11	1.6	72	2	0.3	7	blanco	30 37
BB070	43.31	-126.01	1.6	76	3	0.2	3	blanco	28 30 33
BB090	43.37	-126.66	0.8	74	4	0.1	2	blanco	28 30 36 37
BB120	43.98	-127.30	0.7	78	3	0.2	13	blanco	28 33 36
BB130	43.64	-127.47	0.5	70	5	0.2	10	blanco	28 30 33 35 36
BB140	43.42	-127.69	1.0	-88	1	0.7	32	blanco	36
BB150	43.31	-127.35	0.7	-84	1	0.8	33	blanco	36
BB170	43.14	-127.78	1.0	-29	1	0.5	20	blanco	36
BB180	42.87	-128.30	1.2	-27	4	0.3	7	blanco	30 33 34 36
BB200	43.49	-127.96	0.7	-90	2	0.2	9	blanco	28 36
BB230	43.57	-128.26	0.7	-86	4	0.1	5	blanco	28 36 38 43
BB240	43.43	-128.36	2.7	-52	3	0.4	1	blanco	28 31 43
BB260	43.62	-128.86	1.7	-21	4	0.2	4	blanco	27 30 32 33
BB290	43.63	-128.51	1.2	-70	3	0.2	6	blanco	28 33 38
BB300	43.84	-128.32	0.7	82	3	0.2	6	blanco	30 34 38
BB320	44.17	-128.71	1.5	84	3	0.3	4	blanco	28 37 42
BB330	44.61	-128.60	0.7	70	5	0.1	6	blanco	28 31 34 38 44
BB350	43.99	-129.08	1.1	-60	4	0.2	2	blanco	28 31 37 42
BB370	43.78	-129.39	0.9	-37	4	0.1	5	blanco	30 33 37 38
BB390	43.99	-129.68	0.6	-37	2	0.2	11	blanco	36 42
BB410	43.93	-130.00	0.8	-52	4	0.1	5	blanco	30 33 37 38
BB420	43.63	-130.21	1.0	-58	5	0.1	5	blanco	30 32 36 37 38
BB440	44.21	-130.46	0.7	-64	3	0.1	7	blanco	28 36 38
BB450	44.23	-130.77	0.6	-70	3	0.2	12	blanco	30 36 38
BB480	44.35	-130.02	0.8	-78	3	0.1	5	blanco	28 36 38
BB510	44.31	-129.34	0.7	-78	5	0.1	5	blanco	30 31 33 36 38
BB530	44.55	-129.82	1.4	-84	3	0.1	3	blanco	28 31 36
BB540	44.59	-130.19	1.1	-74	5	0.1	2	blanco	28 30 34 36 38
BB550	44.68	-130.62	0.5	-39	2	0.3	22	blanco	36 44
G37B	42.59	-127.72	1.1	-66	10	0.1	1	blanco	25 26 28 30 33 34 36 37 38 44
J06Stack	43.25	-128.80	0.8	-37	5	0.2	9	blanco	6 13 14 36 37
FS01B	40.33	-124.95	1.4	-72	4	0.2	3	gorda	24 34 37 38 41
FS02B	40.35	-124.80	1.5	-21	2	0.4	9	gorda	30 33
FS04B	40.24	-124.51	NA	NA	0	NA	NA	gorda	NA
FS05B	40.39	-124.90	NA	NA	0	NA	NA	gorda	NA
FS06B	40.38	-124.79	NA	NA	0	NA	NA	gorda	NA
FS07B	40.34	-124.66	1.8	-60	1	0.4	10	gorda	36
FS09B	40.44	-124.81	NA	NA	0	NA	NA	gorda	NA
FS11B	40.43	-124.58	1.1	-37	1	0.6	24	gorda	36

FS12B	40.44	-124.51	NA	NA	0	NA	NA	gorda	NA
FS13B	40.49	-124.81	NA	NA	0	NA	NA	gorda	NA
FS14B	40.50	-124.59	NA	NA	0	NA	NA	gorda	NA
FS15B	40.49	-124.51	NA	NA	0	NA	NA	gorda	NA
FS18B	40.57	-124.50	NA	NA	0	NA	NA	gorda	NA
FS19B	40.63	-124.47	NA	NA	0	NA	NA	gorda	NA
FS20B	40.39	-125.03	NA	NA	0	NA	NA	gorda	NA
G02B	40.05	-125.30	1.4	-78	5	0.2	4	gorda	28 30 36 37 38
G03Stack	40.06	-126.16	2.2	-35	2	0.3	5	gorda	11 36
G05B	40.07	-127.75	1.6	-80	3	0.2	2	gorda	30 36 38
G10B	40.68	-125.55	1.2	-72	9	0.1	1	gorda	28 30 33 36 37 38 39 41 44
G11B	40.69	-126.38	1.8	-80	2	0.3	4	gorda	30 36
G12B	40.69	-127.23	1.2	-74	1	1.0	35	gorda	27
G13B	40.68	-128.03	1.3	-76	4	0.2	3	gorda	28 33 36 37
G19B	41.31	-125.77	1.2	-74	3	0.1	2	gorda	23 28 36
G20B	41.30	-126.61	1.4	-76	6	0.1	2	gorda	28 30 33 36 37 38
G21B	41.42	-127.45	1.2	-70	4	0.2	4	gorda	27 36 37 38
G22B	41.31	-128.27	1.1	-66	3	0.1	5	gorda	28 36 38
G28B	41.94	-126.73	1.5	-62	7	0.1	2	gorda	28 29 30 32 36 42 43
G29B	41.98	-127.48	1.1	-68	4	0.1	3	gorda	28 33 36 37
G30Stack	41.96	-128.32	1.6	-76	3	0.4	11	gorda	6 33 36
G36B2	42.60	-126.90	1.4	-80	5	0.2	3	gorda	28 30 33 38 40
J09B	40.20	-124.73	0.9	9	1	0.5	25	gorda	36
G27B	41.92	-126.02	1.5	86	3	0.1	2	jdf	28 38 42
G35B	42.57	-126.06	1.8	76	2	0.2	4	jdf	25 38
J11B	43.54	-126.37	0.8	64	5	0.1	5	jdf	25 30 36 37 38
J19B	44.18	-126.27	0.6	66	5	0.1	5	jdf	25 28 30 36 38
J20B	44.35	-127.10	0.8	62	5	0.1	2	jdf	28 30 33 36 38
J21C	44.53	-128.04	1.7	78	2	0.5	6	jdf	48 55
J27B	44.85	-126.31	1.2	74	3	0.3	7	jdf	23 33 36
J28Stack	45.06	-127.16	1.2	74	7	0.2	2	jdf	18 28 33 36 48 56 58
J29Stack	45.18	-128.01	1.1	58	4	0.1	2	jdf	13 18 45 51
J30Stack	45.42	-128.91	0.8	52	8	0.1	3	jdf	4 5 6 14 45 46 48 51
J35Stack	45.50	-126.27	1.1	62	12	0.1	3	jdf	1 6 7 8 12 17 18 21 45 48 56 58
J36Stack	45.69	-127.12	0.9	56	9	0.1	2	jdf	1 2 15 21 45 48 51 52 58
J37Stack	45.86	-127.99	0.6	78	6	0.1	6	jdf	6 13 18 45 51 58
J38Stack	46.04	-128.85	0.6	56	5	0.1	9	jdf	6 10 12 13 56
J43Stack	46.14	-126.17	0.8	72	14	0.1	3	jdf	1 3 6 7 9 19 20 21 45 47 51 52 55 58
J44Stack	46.32	-127.04	0.9	64	6	0.1	4	jdf	1 6 9 45 51 58
J45Stack	46.52	-127.90	1.0	68	3	0.4	11	jdf	6 13 48 51 56 58
J46Stack	46.66	-128.79	0.6	13	11	0.1	3	jdf	6 12 13 19 45 46 47 48 54 56 58

J51A	46.80	-126.16	0.7	50	4	0.2	6	jdf	6	17	20	21									
J52Stack	46.99	-127.02	0.8	74	5	0.1	5	jdf	6	13	47	50	51								
J53Stack	47.16	-127.92	0.7	66	5	0.1	5	jdf	6	47	53	56	58								
J59Stack	47.51	-126.42	0.6	54	5	0.1	7	jdf	1	21	22	47	58								
J61Stack	47.87	-128.20	1.2	58	8	0.1	2	jdf	6	12	13	46	47	48	49	53					
J67Stack	48.15	-127.08	1.0	56	11	0.1	3	jdf	5	6	12	13	15	17	45	47	51	52	58		
J68Stack	48.48	-127.83	1.2	54	4	0.1	6	jdf	6	48	51	56									
A04D	48.72	-122.71	0.6	70	4	0.1	4	land	6	30	51	58									
E04D	46.56	-122.57	1.0	76	4	0.1	1	land	28	30	36	38									
I04D	43.79	-122.41	1.9	64	4	0.1	2	land	6	30	36	38									
K02D	42.70	-123.67	1.8	46	4	0.1	1	land	6	30	36	51									
O02D	40.18	-121.80	0.9	44	4	0.1	8	land	6	30	33	37									
J48Stack	47.13	-130.64	1.5	-74	3	0.2	2	pacific	30	37	51										
J63Stack	48.21	-130.00	0.8	-64	10	0.1	4	pacific	12	14	25	26	30	33	36	47	51	58			
J23Stack	44.84	-129.68	0.7	-80	7	0.1	4	ridge	12	26	30	36	38	45	51						
J31Stack	45.55	-129.67	0.7	68	5	0.2	10	ridge	13	14	45	51	56								
J32C	45.71	-130.60	1.5	-11	2	0.3	5	ridge	48	56											
J39Stack	46.18	-129.64	0.8	5	10	0.1	4	ridge	6	7	9	14	47	48	51	53	56	58			
J47Stack	46.84	-129.71	0.8	33	7	0.1	2	ridge	6	9	13	45	53	57	58						
J54Stack	47.34	-128.81	0.6	-7	4	0.2	15	ridge	7	10	48	51									
J55Stack	47.53	-129.71	1.2	-37	1	1.0	25	ridge	6												
J69C	48.63	-128.74	1.4	52	2	0.2	3	ridge	51	58											
FN01C	46.88	-124.33	NA	NA	0	NA	NA	subduction	NA												
FN02C	46.95	-124.43	NA	NA	0	NA	NA	subduction	NA												
FN03C	46.89	-124.53	NA	NA	0	NA	NA	subduction	NA												
FN04C	46.92	-124.60	NA	NA	0	NA	NA	subduction	NA												
FN05Stack	46.86	-124.66	NA	NA	0	NA	NA	subduction	NA												
FN07Stack	46.86	-124.79	NA	NA	0	NA	NA	subduction	NA												
FN08Stack	46.89	-124.88	NA	NA	0	NA	NA	subduction	NA												
FN09C	46.84	-124.89	NA	NA	0	NA	NA	subduction	NA												
FN10C	46.90	-124.99	NA	NA	0	NA	NA	subduction	NA												
FN11C	46.82	-125.05	NA	NA	0	NA	NA	subduction	NA												
FN12Stack	46.89	-125.12	NA	NA	0	NA	NA	subduction	NA												
FN13C	47.00	-125.30	1.0	66	2	0.2	6	subduction	56	59											
FN14Stack	46.02	-124.96	1.3	31	2	0.2	2	subduction	1	20											
FN16A	46.80	-125.52	1.3	80	3	0.3	6	subduction	1	6	13										
FN18A	46.70	-124.72	1.4	90	2	0.5	9	subduction	1	6											
FN19C	46.73	-124.37	NA	NA	0	NA	NA	subduction	NA												
G09B	40.66	-124.72	NA	NA	0	NA	NA	subduction	NA												
G17B	41.28	-124.34	NA	NA	0	NA	NA	subduction	NA												
G18B	41.30	-124.94	NA	NA	0	NA	NA	subduction	NA												

G25B	41.92	-124.59	1.7	74	3	0.3	1	subduction	30 36 37
G26B	41.92	-125.18	1.4	74	1	0.8	21	subduction	37
G34B	42.56	-125.20	2.4	72	2	0.4	6	subduction	30 33
J10B	43.35	-125.54	1.6	76	4	0.2	2	subduction	28 33 37 38
J17B	43.79	-124.61	NA	NA	0	NA	NA	subduction	NA
J18B	44.01	-125.47	1.2	70	6	0.1	1	subduction	28 30 36 37 38 43
J25Stack	44.47	-124.62	1.2	46	2	0.4	15	subduction	1 2
J26C	44.65	-125.47	0.9	58	2	0.6	23	subduction	47 58
J33Stack	45.11	-124.57	1.1	50	5	0.2	6	subduction	6 13 20 36 51
J34C	45.31	-125.42	NA	NA	0	NA	NA	subduction	NA
J41Stack	45.81	-124.54	1.9	25	2	0.3	5	subduction	1 58
J42C	45.93	-125.30	1.7	54	1	0.4	12	subduction	56
J49Stack	46.44	-124.43	NA	NA	0	NA	NA	subduction	NA
J50Stack	46.64	-125.30	0.9	56	7	0.2	6	subduction	1 12 20 21 47 50 58
J57Stack	47.08	-124.45	NA	NA	0	NA	NA	subduction	NA
J58Stack	47.32	-125.58	1.2	70	5	0.3	7	subduction	13 14 20 50 59
J65Stack	47.89	-125.14	NA	NA	0	NA	NA	subduction	NA
J73Stack	48.77	-126.19	NA	NA	0	NA	NA	subduction	NA
M01Stack	49.15	-126.72	NA	NA	0	NA	NA	subduction	NA
M02C	48.31	-125.60	NA	NA	0	NA	NA	subduction	NA
M03Stack	47.89	-126.10	1.4	66	4	0.1	2	subduction	6 47 50 53
M04C	45.56	-125.19	1.7	76	2	0.4	2	subduction	48 58
M05C	46.17	-124.93	2.1	76	1	0.6	5	subduction	58
M06C	45.53	-124.93	1.6	-9	1	0.9	9	subduction	58
M07A	44.90	-125.12	1.9	17	5	0.3	4	subduction	1 4 8 16 20
M08Stack	44.12	-124.90	NA	NA	0	NA	NA	subduction	NA
M09B	44.25	-125.06	1.0	48	1	0.6	18	subduction	23
M11B	42.93	-125.02	1.5	52	2	0.4	13	subduction	30 32
M12B	42.18	-124.95	NA	NA	0	NA	NA	subduction	NA
M14B	40.99	-124.59	0.4	-88	4	0.2	19	subduction	27 28 30 36

Table DR1: Summary of the stacked splitting observations for results shown in Figs. 2 and 3. Sites reporting a single year of data retain the original station name; sites reporting multiple years of data are followed by 'stack'. Uncertainties are reported at the one-sigma level of confidence; same as Fig. 3. Event IDs refer to Table DR2.

ID #	year	day	hour	min	sec	mag	Lat	Lon	depth	# used
1	2011	296	10	41	23	7.1	38.7	43.5	16	12
2	2011	306	14	59	28	6.2	-55.3	-128.8	10	2
3	2011	318	4	5	11	6.4	-1.0	126.9	17	1
4	2011	334	0	27	7	6.0	15.5	119.0	9	1
5	2011	341	22	23	10	6.1	-27.9	-70.9	20	2
6	2011	348	5	4	59	7.1	-7.6	146.8	141	18
7	2012	10	18	36	59	7.2	2.4	93.2	19	4
8	2012	15	13	40	20	6.6	-61.0	-56.1	8	2
9	2012	37	3	49	13	6.7	10.0	123.2	11	4
10	2012	37	10	10	20	6.0	9.9	123.1	9	2
11	2012	80	17	56	19	6.3	-3.8	140.3	66	1
12	2012	81	22	15	6	6.6	-6.2	146.0	118	8
13	2012	85	22	37	6	7.1	-35.2	-72.2	41	13
14	2012	102	8	38	37	8.6	2.3	93.1	20	6
15	2012	105	10	56	19	6.2	-57.7	-65.3	15	1
16	2012	106	5	57	40	6.3	2.6	90.3	25	1
17	2012	108	3	50	16	6.7	-32.6	-71.4	29	3
18	2012	108	7	13	49	6.9	-5.5	147.1	198	4
19	2012	112	1	25	13	6.0	-1.6	134.2	17	2
20	2012	149	5	7	23	6.7	-28.0	-63.1	587	7
21	2012	175	4	34	53	6.1	3.0	97.9	95	5
22	2012	185	10	36	16	6.3	-40.0	173.8	230	1
23	2012	244	12	47	33	7.6	10.8	126.6	28	3
24	2012	247	18	23		6.3	-10.7	113.9	14	1
25	2012	258	4	51	47	6.3	-3.3	100.6	19	5
26	2012	282	11	43	31	6.2	-4.5	129.1	10	3
27	2012	286	0	31	28	6.6	-4.9	134.0	13	3
28	2012	316	1	12	39	6.9	23.0	95.9	14	17
29	2012	342	18	19	6	6.3	-38.5	176.1	163	1
30	2012	345	16	53	8	7.1	-6.5	129.8	155	20
31	2013	30	20	15	43	6.8	-28.1	-70.7	45	4
32	2013	47	4	37	36	6.2	5.8	125.8	105	2
33	2013	96	4	42	36	7.0	-3.5	138.5	66	14
34	2013	99	11	52	50	6.3	28.4	51.6	12	3
35	2013	104	1	32	22	6.5	-6.5	154.6	31	1
36	2013	106	10	44	20	7.7	28.0	62.0	80	30
37	2013	106	22	55	27	6.6	-3.2	142.5	13	15
38	2013	110	0	2	48	6.6	30.3	102.9	14	17
39	2013	131	2	8	9	6.2	26.6	57.8	15	1
40	2013	140	9	49	5	6.3	-44.9	-80.8	10	1
41	2013	153	5	43	4	6.3	23.8	121.1	17	2
42	2013	164	16	47	23	6.6	-10.0	107.2	9	2
43	2013	166	11	20	36	6.0	-33.9	179.4	195	2
44	2013	166	16	11	3	6.3	34.4	25.0	10	2
45	2013	228	2	31	6	6.5	-41.7	174.2	8	12
46	2013	244	11	52	30	6.5	-7.4	128.2	112	3
47	2013	267	11	29	48	7.8	27.0	65.5	15	12
48	2013	271	7	34	7	6.8	27.3	65.6	15	13

49	2013	273	5	55	56	6.4	-30.9	-178.4	42	1
50	2013	284	21	25	0	6.2	-30.7	-178.5	151	4
51	2013	285	13	11	53	6.8	35.5	23.3	40	18
52	2013	288	0	12	2	7.1	9.9	124.1	19	4
53	2013	304	23	3	59	6.5	-30.3	-71.6	29	5
54	2013	320	3	34	31	6.9	-60.3	-47.1	10	1
55	2013	321	9	4	55	7.8	-60.3	-46.4	10	2
56	2013	335	1	24	14	6.5	-7.0	128.4	10	12
57	2014	33	9	26	38	6.4	-32.9	-177.9	44	1
58	2014	43	9	19	49	6.9	35.9	82.6	10	22
59	2014	174	19	19	16	6.9	-30.0	-177.7	20	2

Table DR2: List of the events used in this study. Plots of the events by back azimuth are shown in Fig. DR2.

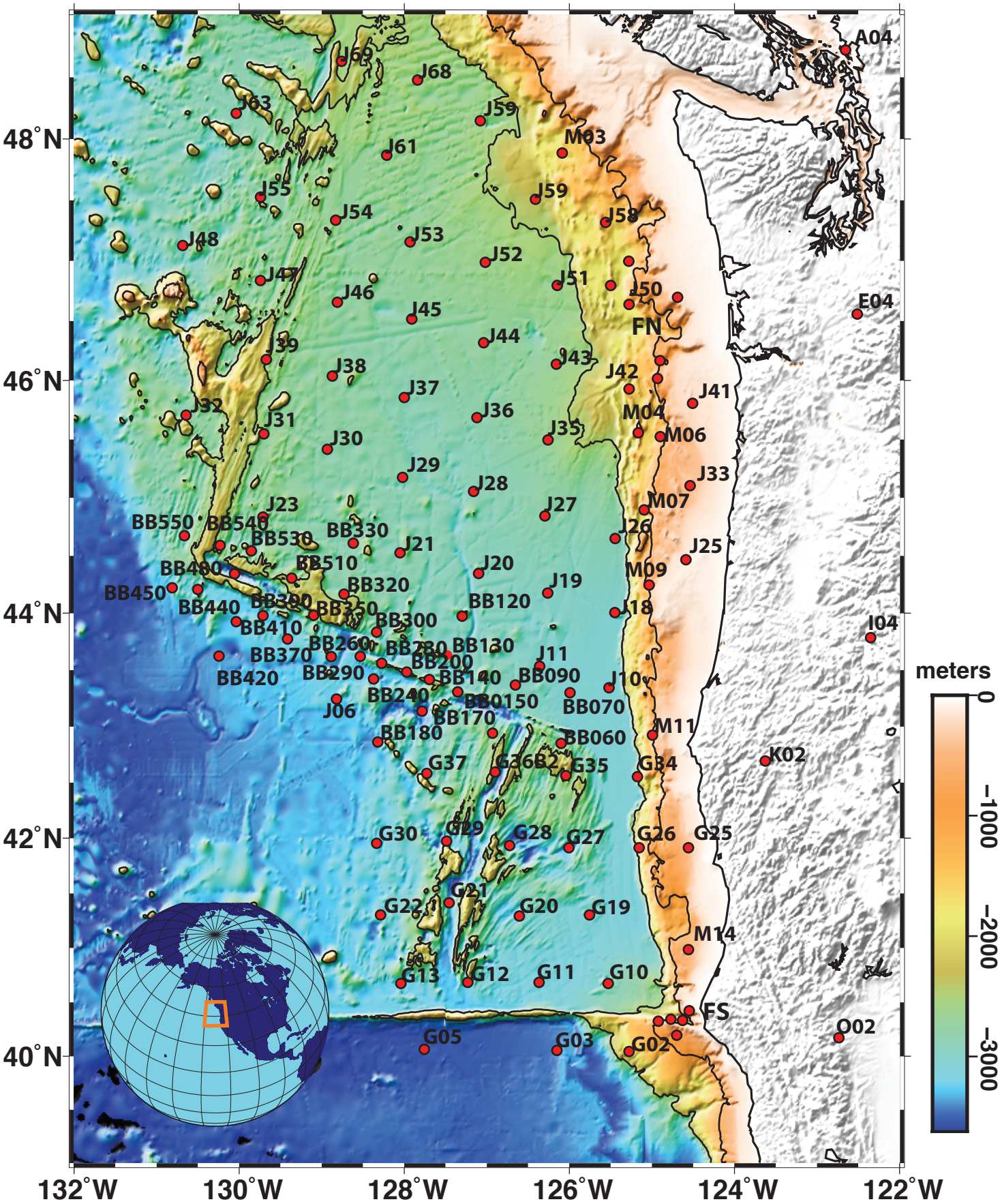

Fig. DR1: Bathymetric map showing stations used in this study (red circles) along with site names.

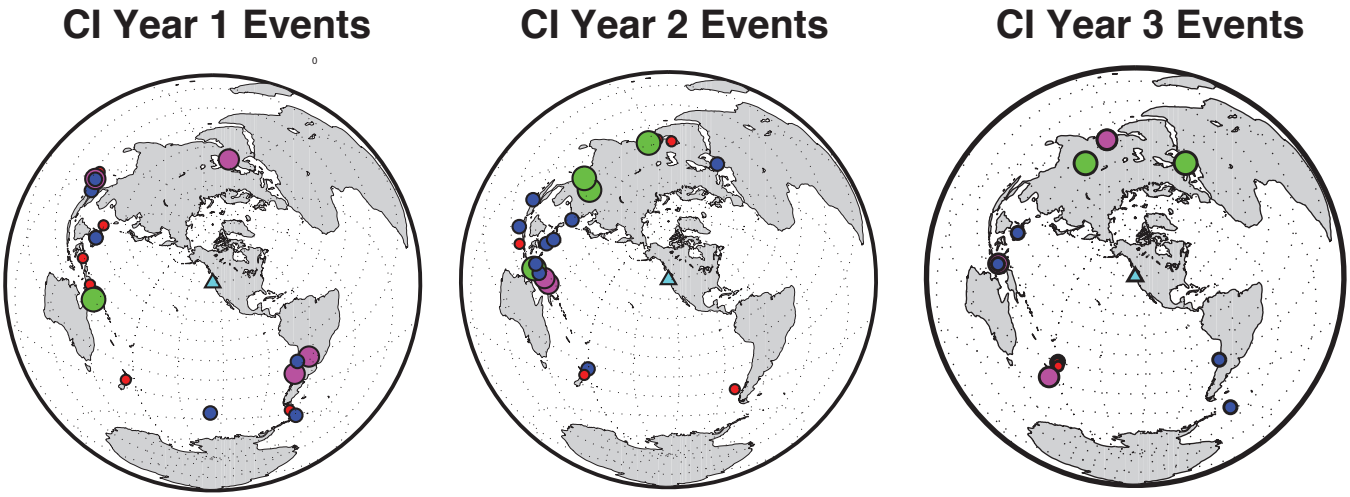

Fig.DR2: Distribution of events by back azimuth. Color and size of a circle corresponds to the number of stations that used a particular event: red = 1-2; blue = 3-5; magenta = 6-15; green = 16 or more. Each panel corresponds to one year of the Cascadia Initiative. Results obtained from the Blanco array used a subset of the events shown in year 1 and 2 panels.

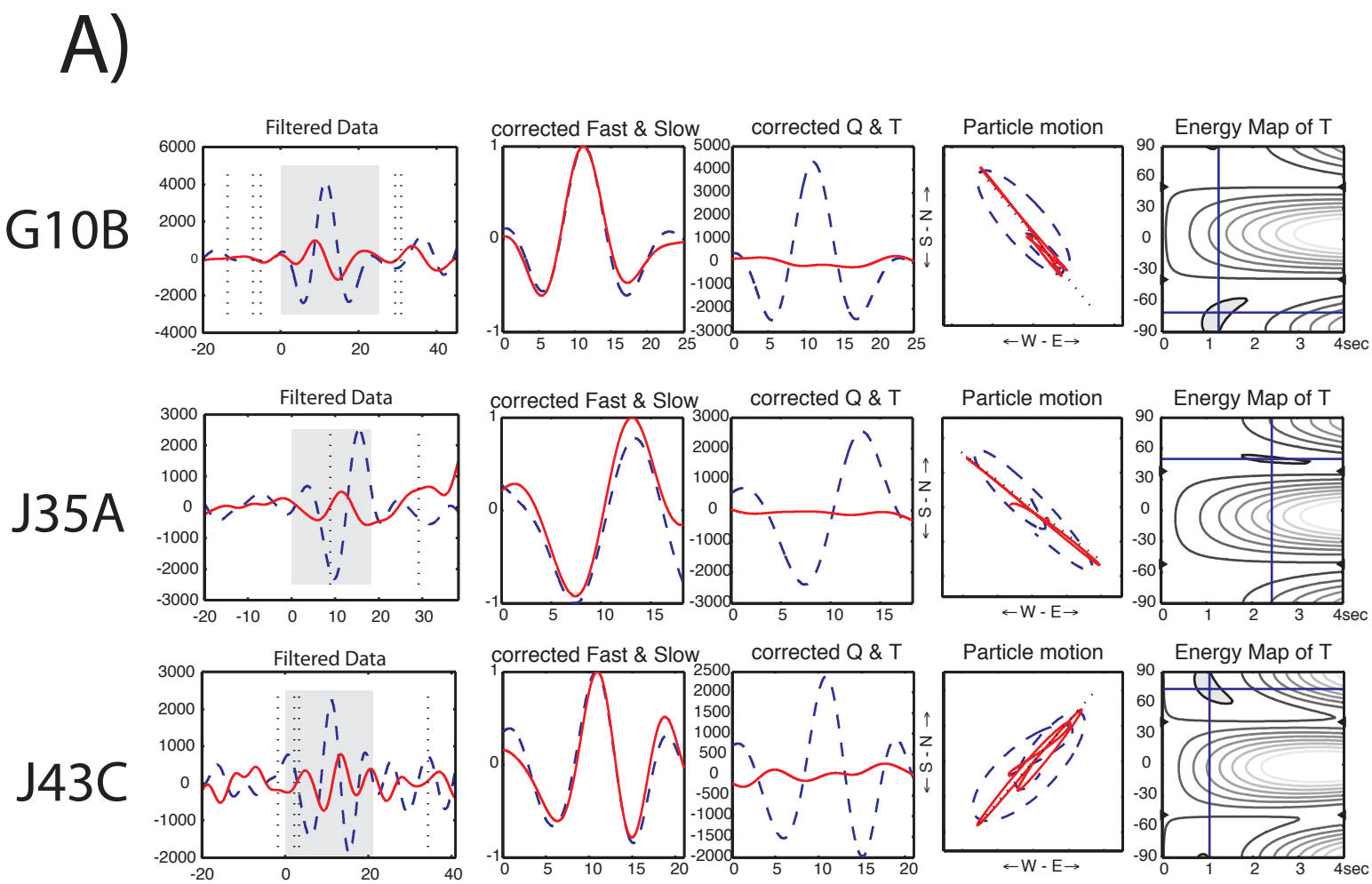

Fig. DR3: Examples of the data used in this study. A) Splitting measurements from G10B, J35A, and J43C. From left to right: i) filtered waveforms in the radial (blue dashed) and transverse (red) directions. Grey band indicates data used for a splitting measurement. ii) The waveforms after correcting for splitting in the fast (blue dashed) and slow (red) directions normalized by peak amplitude. iii) Corrected waveforms in the radial (blue dashed) and transverse (red) directions. iv) Particle motion before (blue dashed) and after (red) correcting for splitting. v) Energy map of the transverse channel produced by grid searching the fast polarization-delay time parameter space. The minimum is marked by the blue crosshairs and the gray region represents the 95% confidence interval. B) The transverse energy maps used to calculate the splitting parameters for station G37B (panels 1 to 10); 95% confidence interval for a single measurement is shown in red. These energy maps are normalized and stacked to produce the final map (panel 11).

B)

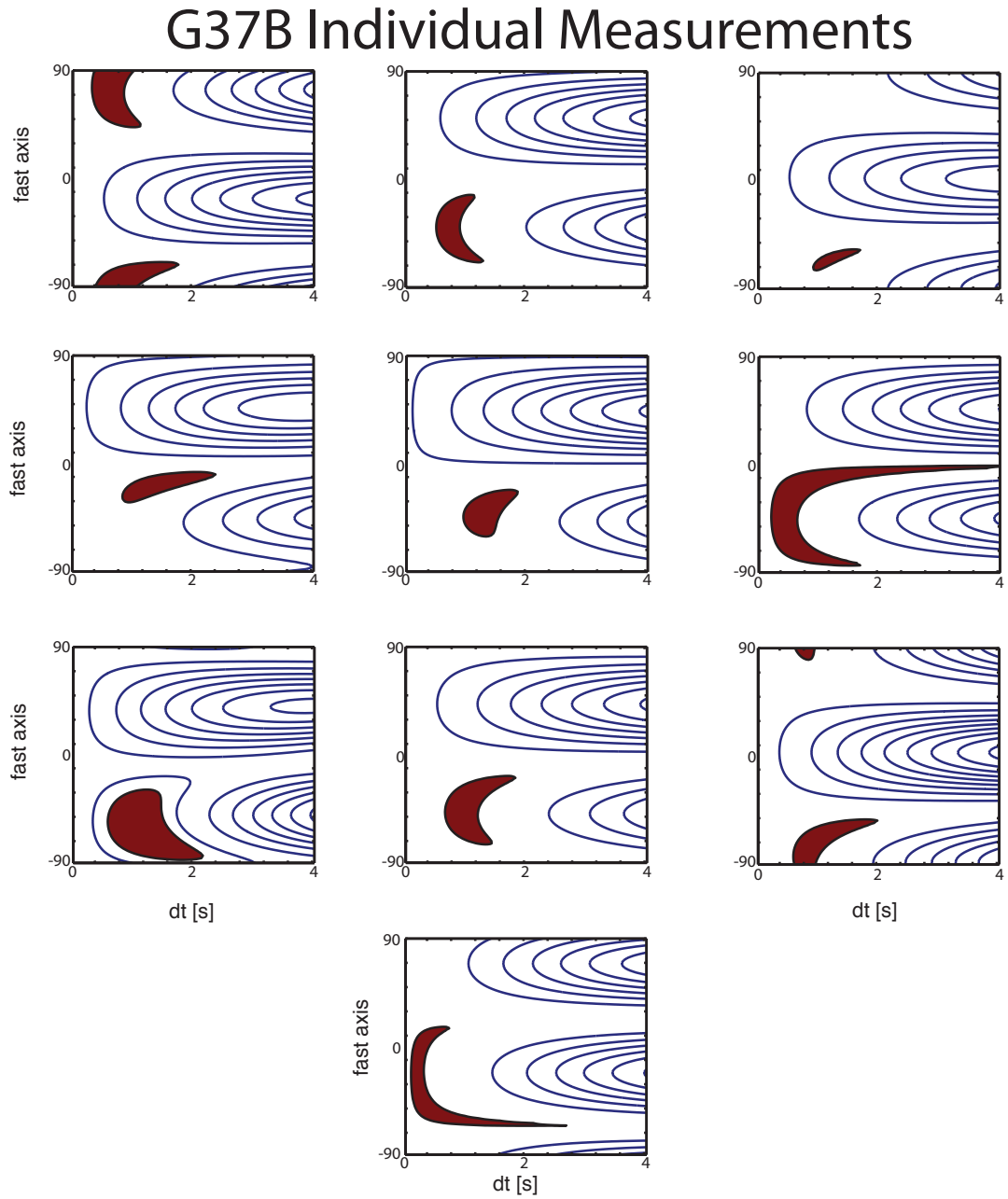
G37B Individual Measurements
fast axis
dt [s]
90
0
-90
0
2
4

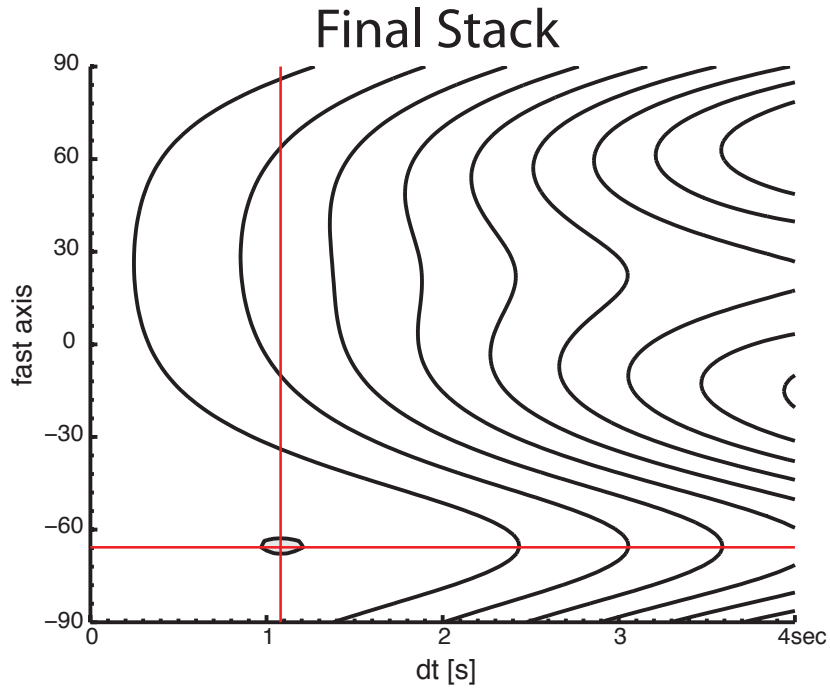
Final Stack
fast axis
dt [s]
90
60
30
0
−30
−60
−90
0
1
2
3
4sec

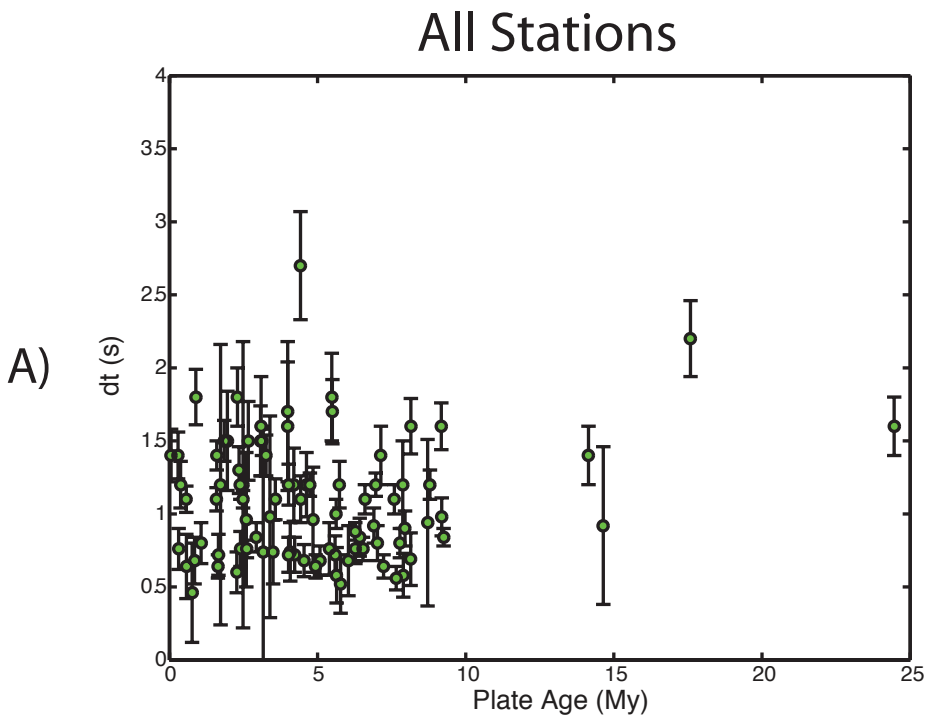

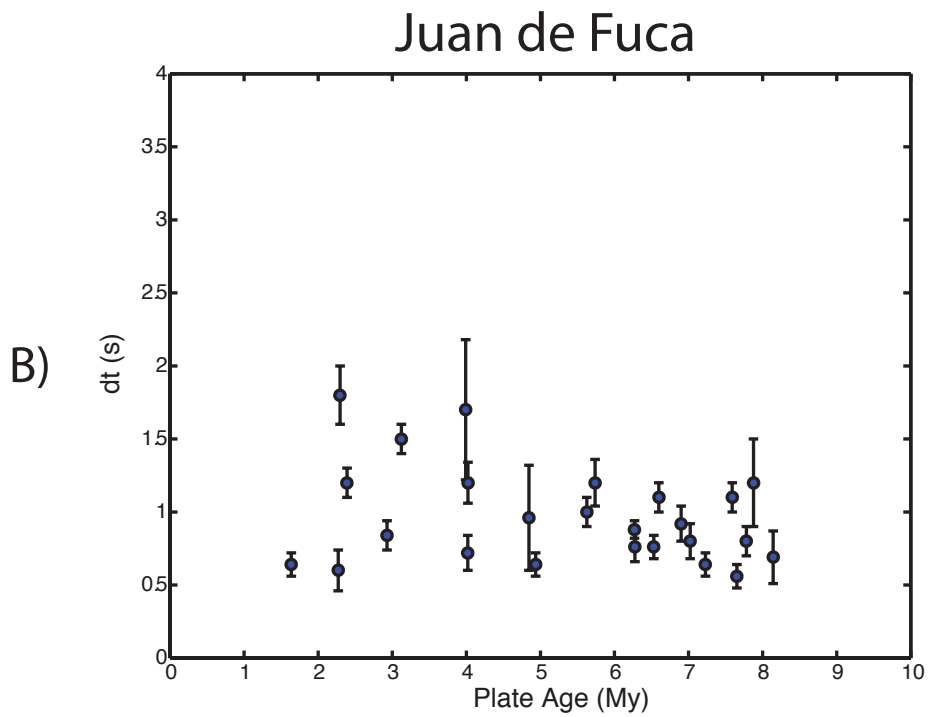

Fig. DR4: Observed delay times plotted by plate age for A) all OBSs used in this study and B) the subset of sites within the interior of the Juan de Fuca plate. Neither plot displays an age dependence.

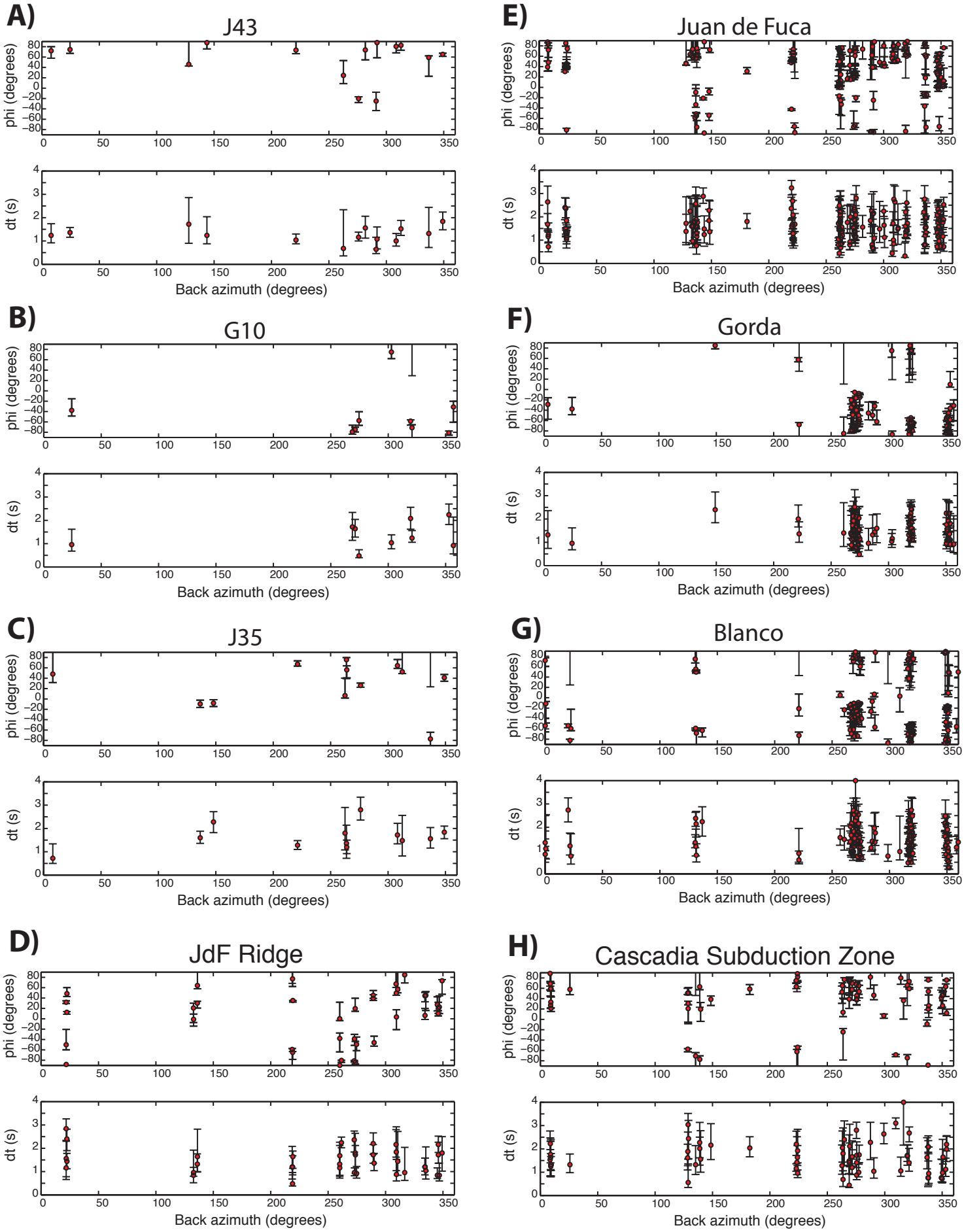

Fig. DR5: Results of individual measurements as a function of back azimuth for selected stations (J43, G10, and J35) and for each tectonic zone defined in Fig. 1. The presence of multiple anisotropic layers is predicted to produce splitting parameters that are dependent on back azimuth (see Fig. DR6). Results for individual stations and for tectonic zones are not adequate to identify a dependence on back azimuth. For each tectonic zone, the individual measurements generally cluster around the average obtained by stacking error surfaces.

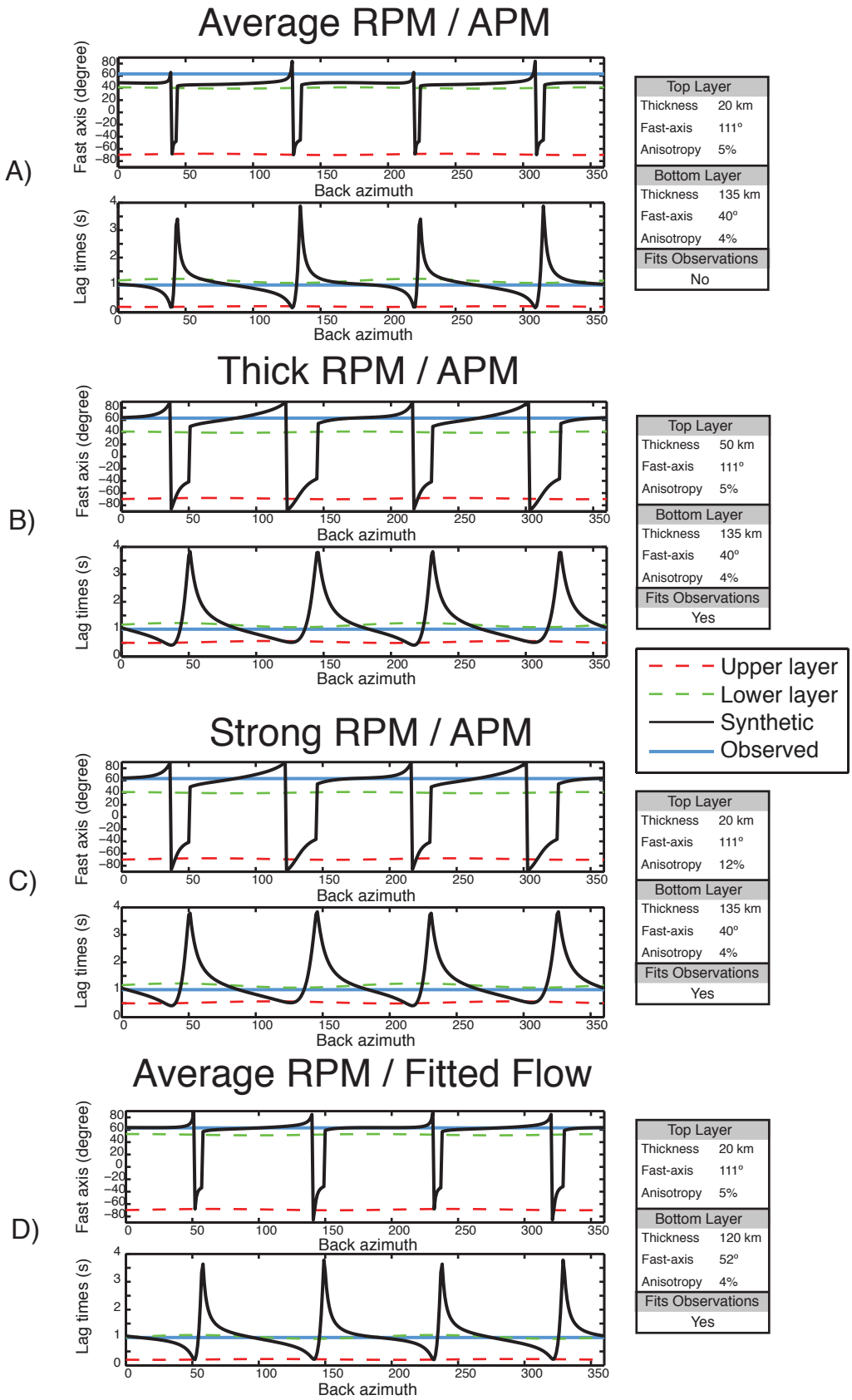

Fig. DR6: Predicted splitting parameters plotted by back azimuth for several two-layer models of anisotropy. Predictions are made using methodology of (Silver and Savage, 1994) and the MSAT software package (Walker and Wookey, 2012). Red and green dashed lines show contributions of upper and lower layers, respectively. Solid black line is the predicted apparent splitting parameter, which is the result of interactions in both layers. Solid blue line shows the average splitting parameters observed for sites located within the Juan de Fuca plate. Model parameters are provided to the right of each panel. A) Model with a 20-km-thick upper layer aligned with RPM and a 135-km-thick lower layer aligned with APM. The thickness of the top layer (20 km) is typical for the JdF plate, which varies between 5 and 30 km. This model does not fit the fast polarization observations (rotated ~15-20°). B) Model with a 50-km-thick upper layer aligned with RPM and a 135-km-thick lower layer aligned with APM. This model fits the observations. C) Model with a highly anisotropic (12% in 20 km) upper layer aligned with RPM and a 135-km-thick lower layer aligned with APM. This model fits the observations. D) Model with a 20-km-thick upper layer (5% anisotropic) aligned with RPM and a 120-km-thick lower layer with fast axis at N52°E. This model fits the observations. See text for discussion.